Master's Thesis

Photoinduced changes in phytochromes studied by means of low temperature UV-Vis spectroscopy

Maryna Goncharenko

University of Jyväskylä
The Department of Biological and Environmental Science
Cell and Molecular Biology
27.02.2018

PREFACE

This research project was done at the Department of Biological and Environmental Science at the University of Jyväskylä during the first half of the year 2016. I would like to thank my supervisor Janne Ihalainen for possibility to join his research group and assistance in changing my major towards cell and molecular biology, which gave me the opportunity to make a research on the border of biology and physical chemistry. I would also like to thank Alli Liukkonen for her great help, advise and patience in the lab, especially during protein expression part of my master's thesis. Many thanks to Dr. Heikki Häkkänen for helping with the spectroscopy measurements, LEDs adjusting and home-built setup assembling. I would also like to thank Jussi Ahokas and Pasi Myllyperkiö for consulting me during the cryostat assembling and testing. I also acknowledge Heikki Takala for providing ready DNA sequences of the mutants used in my work. The last, but not least, great thanks to the Nanoscience Centre for providing me with opportunity to realize all my research ideas using extensive scientific facilities.

University of Jyväskylä
Faculty of Mathematics and Science

Abstract of Master's thesis

Author: Maryna Goncharenko
Title of thesis: Photoinduced changes in phytochromes studied by means of low temperature UV-Vis spectroscopy
Finnish title: Valoindusoituja muutoksia fytokromeissa – matalan lämpötilan UV-Vis spektroskopiaa hyväksi käyttäen

Date: 27.02.2018 **Pages:** 36 + 1

Department: Department of Biological and Environmental Science
Chair: Cell and Molecular Biology
Supervisors: Janne Ihalainen

Abstract:

Phytochromes are a major family of red-light-sensing kinases that control diverse cellular functions in plants, bacteria and fungi. These proteins must relay structural signals from the sensory site over large distances to regulatory output domains. To accomplish this function, they undergo rather large structural changes from one state to another. The general aim of this work was to study these structural changes and possible protonation states of the photosensory core of the bacteriophytochrome from *Deinococcus radiodurans* in the intermediate states of the photoreaction, which became possible to observe under low temperatures. Moreover, it was interesting to investigate the role Serine272 in stabilization of both states of the photoreaction. Albeit a large amount of spectroscopic studies, the exact mechanism of the photoreaction remains unclear. This question was addressed by recording absorption spectra of studied phytochrome with the help of UV-Vis spectroscopy performed under low temperatures. To understand the role of Serine272 a site-selective mutation in studied bacteriophytochrome was performed.

Purified and concentrated phytochromes were analyzed using SDS-PAGE and UV-Vis spectroscopy methods. Furthermore, an approach to measure UV-Vis spectra at low temperatures was developed. The temperature ranges that can be used to trap phytochromes in the intermediate states of the photocycle were identified.

Spectroscopy studies revealed that mutated phytochrome could adopt two reversible states when illuminated with far red and near far red light. This finding contradicted the initial hypothesis about potential effect of serine272 on the stability of the photocycle and the photoreversibility of the process. Low temperature UV-Vis measurements confirmed hypothesis that it is possible to trap the protein in different intermediate states of its photocycle, thereby control the whole process by keeping the temperature at the appropriate level.

Keywords: phytochrome, *Deinococcus radiodurans*, intermediates, low temperature UV-Vis spectroscopy, photocycle

TABLE OF CONTENTS

ABBREVIATIONS

BV	biliverdin IXα - a linear tetrapyrrole, metabolically derived from heme
BphP	member of the bacteriophytochrome subfamily
CBD	chromophore-binding domain
Cph1, Cph2	phytochrome subfamilies named after cyanobacterial phytochromes 1 and 2
Fph	member of the fungal phytochrome subfamily
FTIR	Fourier transform infrared spectroscopy
HKRD	histidine kinase related domain
GAF	phosphodiesterase - adenylate cyclase – FhlA
IPTG	isopropyl β-D-1-thiogalactopyranoside
LB	Luria Bertani
NiNTA	nickel-nitrilotriacetic acid
OD	optical density
PAS	Per/Arnt/Sim domain
Phy	member of the plant phytochrome subfamily
PHY	phytochrome-spesific domain
Pr	red-light-absorbing phytochrome state
Pfr	far-red-light- absorbing phytochrome state
RT	room temperature
SDS-PAGE	sodium dodecyl sulfate-polyacrylamide gel electrophoresis
SEC	size-exclusion chromatography
UV-Vis	ultraviolet-visible light

1. INTRODUCTION

1.1. General information and history of phytochromes discovery

Sensing light and responding to it is essential for all living organisms. Such ability helps them to transmit physical signals into biochemical outputs and thus adapt their metabolism to the light environment. Scientific interest of how exactly plants can sense and correctly respond to light has been a driver in discovery of proteins involved in photosensory pathways.

Extensive research showed that in order to adopt their behaviour to the incident light, plants utilize a lot of different photosensory proteins, called phytochromes, that are able to perceive a range of wavelengths (Batschauer 2003, Briggs and Spudich 2005, Schafer and Nagy 2005). Phytochromes are large proteins representing extensive family of red and far-red light sensing photoreceptors. They are critical regulators in key adaptive processes, such as photomorphogenesis, shade avoidance, seed germination, as well as flowering timing in higher plants (Butler 1959, Sage 1992, Rockwell 2006, Rockwell 2010, Franklin and Quail 2010, Auldridge and Forest 2011).

Phytochromes were firstly identified in 1959 by researchers Bulter and Siegelman, who discovered that red light was vital for triggering flowering responses (Butler 1959). Researchers also found that these responses were reversible once the object of interest was illuminated with far-red light, indicating the presence of a photoreversibility. Later in 1996, the first evidence of phytochromes outside the plant kingdom was obtained, when gene of the cyanobacterium *Synechocystis* was proven to have some similarities with those of plant phytochromes. Thereafter, phytochromes have been discovered in cyanobacteria, nonoxygenic bacteria and fungi (Rockwell 2006). In turned out that in bacteria phytochromes regulate light-protective pigment biosynthesis (Davis 1999). In 2005, Vierstra and Forest published revolutionary paper, where they introduced three-dimensional structure of the photosensory domain of *Deinococcus radiodurans* phytochrome. It revealed that the protein chain forms uncommon structure for a protein. This finding became the basis of phytochrome signalling in plants used in further studies (Wagner 2005).

Nowadays we consider phytochromes as a large family of light-sensitive signalling proteins, each containing a linear tetrapyrrolic chromophore, which regulate behaviour of plants, bacteria and fungi with respect to changes in their light environment (Pratt 1995).

1.2. Modular domain architecture of BphP and chromophore structure

Profound research of photosensory proteins allowed to classify phytochromes into five subfamilies, namely Phy (members of the plant phytochrome subfamily), BphP (members of the bacteriophytochrome subfamily), Fph (members of the fungal phytochrome subfamily), Cph1 and Cph2 (phytochrome subfamilies named after cyanobacterial phytochromes 1 and 2) (Rockwell 2006). All five subfamilies of phytochromes possess an N-terminal photosensory core region and typically share regulatory output domain. Most phytochromes are dimeric proteins, all having modular domain architecture (Bjorling 2016). In this research work, only bacteriophytochromes will be covered, thus it makes sense to focus entirely on the modular domain architecture of this subfamily.

BphPs consists of a N-terminal photosensory core with three domains (P2 or PAS domain, P3 or GAF domain and P4 or PHY domain) and a C-terminal regulatory histidine kinase related domain (HKRD) (Figure 1). Together PAS and GAF domains are often called CBD (chromophore binding domain). Altogether, bacteriophytochrome consists of PAS-GAF-PHY N-terminal photosensory module combined with C-terminal HKRD module (Rockwell 2006 and 2010). The PAS and GAF domains form stable globular structure due to the trefoil knot formed by the backbone, which possibly establishes more rigid structure than it is usual for ordinary domain interactions (Rockwell 2006, Wagner 2005, Zao 2004). The connection between GAF and PHY domains is established through a helical spine and the so-called PHY-tongue, which changes its conformation from β sheet to α helix when it changes from one state to another (Essen 2008, Yang 2008, Takala 2014).

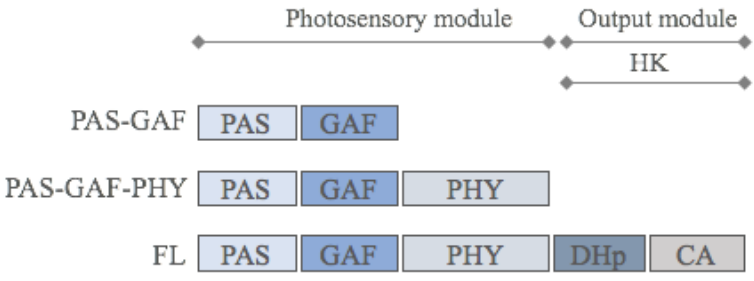

Figure 1: **Domain architecture of bacteriophytochrome constructs.**
Schematic presentation of phytochrome fragments

From the chemical point of view, phytochrome consists of chromophore represented by a single bilin molecule. Light absorption causes changes in this molecule and its hydrogen bonding network that lead to larger structural changes in the whole protein (Takala 2014). This means that characteristic absorbance spectrum of a phytochrome is associated with a covalently attached linear tetrapyrrole bilin chromophore, which enables photoconversion between the two states of phytochrome. The nature of chromophore varies for different subfamilies of phytochromes, namely Phys use phytochromobilin (PΦB), Cph1s and Cph2s use phycocyanobilin (PCB), whereas BphPs and Fphs instead utilize biliverdin IXα (BV) as chromophore (Bhoo 2001). Biliverdin is a green tetrapyrrole bile pigment and in the same manner as other bilin chromophore classes is derived from the oxidative cleavage of heme by a heme oxygenase. Biliverdin is covalently attached to the protein via a thioether linkage between a cysteine residue of the PAS domain and the bilin A-ring (Wagner 2007). The D-ring is not so tightly packed in the protein as compared to other parts of chromophore, making it easier for this ring to rotate during the photoreaction. On the contrary, A-ring of the chromophore is deeply buried inside the GAF domain via covalent linkage to the conserved Cys24 (Rockwell 2006). Thus, we may speak of phytochromes as about photoswitchable photosensors that utilize bilin chromophores.

1.3. Photoreversibility and signal transduction of phytochromes

The key characteristics that helped to understand the role of phytochromes in plans, was reversibility of plant responses upon illumination with corresponding wavelength (Sage 1992). Phytochromes can exist in two states: one that absorbs red light (Pr state with absorbance maximum at 665 nm) and one the absorbs far-red light (Pfr state with absorbance maximum at 785 nm). These states correspond to red light–enriched (full sun) and red light–depleted (shade) conditions respectively. These two states are reversible, with far-red light illumination restoring Pr state, involving both primary photochemistry and subsequent thermal steps (Rudiger and Thummler 1991, Terry 1993, Kendrick 1994).

Phytochromes exhibit a fascinating signal transduction mechanism, where the atomic-scale changes in biliverdin hydrogen-bonding network (biliverdin cis-trans isomerization) upon a photon absorption event, firstly lead to ångstrom-scale distance change in the "tongue" in PHY domain (β-sheet in dark form and to α-helix in illuminated one) and finally transform into nanometer-scale conformational signal in the whole protein (the dimer adopts an open Y-like shape of the PHY domain in illuminated form) (Takala 2014). D-ring

of the chromophore rotates due to Z–E isomerization about the C15–C16 double bond between the C- and D-pyrrole rings of the tetrapyrrole chromophore biliverdin upon excitation with red light (Rudiger 1983, Sineshchekov 1995, Kneip 1999, Gartner 2003, Yang 2009, Dasgupta 2009, Sog 2011, Burgie 2013, Narikawa 2013, Cornilescu 2014). Recent amazing finding, conducted with the help of time-resolved x-ray scattering and crystal structures, discovered that mentioned above biliverdin cis-trans isomerization leads to the large-scale opening of the dimer in the PAS-GAF-PHY fragment. This happens due to refolding of the PHY tongue (antiparallel β-sheet configuration in Pr state changes to α-helix in Pfr state in the region of PHY tongue) (Takala 2014). Further reconnection of the α-helical tongue in the Pfr state with the GAF domain pulls on opposite helical spines to open neighbouring PHY domain. Presumably, this motion is transmitted into the regulatory histidine kinase related domain that initiates downstream signal transduction. Thus, conversion from Pr to Pfr state results in notable structural differences in the phytochrome, and clear ‘open’ and ‘closed’ structures can be distinguished.

1.4. Photocycle of the phytochromes

By now, most of the knowledge about the photocycle of phytochromes has been provided by spectroscopic studies. The photoreaction of the bacterial phytochrome proceeds via three intermediates, usually termed Lumi-R, Meta-Ra, and Meta-Rc (Figure 2). In the Pr state, biliverdin is cationic with all the four pyrrole-ring nitrogens protonated (von Stetten 2007, Kneip 1999, Eilfeld 1978, Spruit and Kendrick 1977). During the first stage of the photocycle towards the first ground state intermediate Lumi-R (absorption maximum at 688 nm), a Z-E isomerization of the biliverdin D-ring between the C15-C16 double bond occurs (Andel 1997, Bischoff 2001). This reaction takes place on the time scale of pico- to nanoseconds. Subsequently, Lumi-R state converts into Meta-Ra within microseconds with absorption maximum at 663 nm (Tu 2005). Meta-Ra intermediate in turn decays in micro- to milliseconds to a deprotonated Meta-Rc intermediate (absorption maximum at 725 nm) leading to D-ring nitrogen deprotonation. Finally, the Meta-Rc photoproduct decays to Pfr on a millisecond time scale in a process that possibly requires reprotonation of the chromophore (Kneip 1999, Andel 1996, Mizutani 1994). Currently, it is assumed that the major conformational change in the protein occurs during Meta-Rc to Pfr transition.

The Pfr state is thermally unstable in most phytochromes: once formed, Pfr will slowly revert nonphotochemically back to Pr in a process known as dark reversion. It can also be

photoconverted almost immediately back to Pr utilizing far-red light. Neither pathway is well understood. Recent interesting study analysed three phytochrome constructs (*Dr*CBD, *Dr*CBD-PHY and *Dr*BphP) with regards to their dark reversion. It revealed that dark reversion of *Dr*CBD is clearly faster than that of longer fragments, whereas *Dr*CBD-PHY exhibits stable photoactivated state (Takala 2014a). Benefits of such stability have proven themselves when crystal structure of *Dr*CBD-PHY photosensory unit in the illuminated state was obtained (Takala 2014b). The photoinduced Pfr-Pr pathway also contains three intermediate steps, namely Lumi-F, Meta-Fa and Meta-Fc (Song 2013, Bjorling 2015). However, this conversion is likely to proceed via a pathway distinct from that for the Pr-Pfr conversion. What differs the backward reaction from the forward one, is that instead of event of protonation or deprotonation, the reformation of D-ring hydrogen bonding occurs. Nevertheless, the detailed process of photoactivation, including the initial release place of the protons, is still under the question (Kneip 1999, Boruki 2001, von Stetten 2006, Bjorling 2016). To get full understanding of the molecular events occurring during the photoreaction, a detailed characterization of the intermediates of both pathways should be in place. Therefore, in this work, difference spectra of mentioned intermediates stabilized at low temperatures have been obtained.

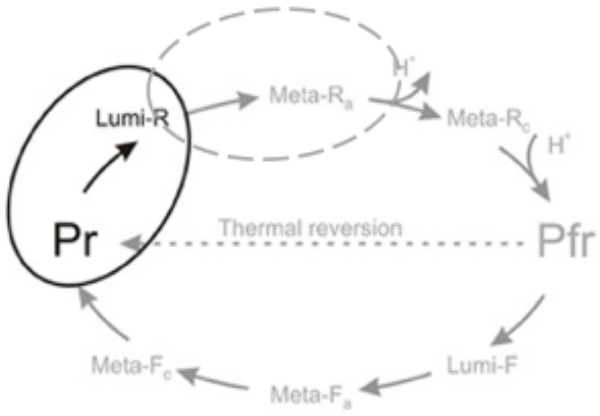

Figure 2: **Complete photocycle of a phytochrome.** The complete photocycle of a phytochrome with its intermediates. Forward reaction proceeds via three intermediates, termed Lumi-R, Meta-Ra, and Meta-Rc. Pfr slowly reverts to Pr, in a process known as dark reversion, or can be photoconverted almost immediately back to Pr through three intermediate steps, named Lumi-F, Meta-Fa and Meta-Fc. Circled are areas of focus of this experiment.

1.5. Absorption spectroscopy

Absorption spectroscopy is a powerful tool used to study protein–protein interactions, as well as protein structures. Different molecules absorb electromagnetic radiation characteristically to their molecular structures which enables us to investigate, for example, secondary structure of proteins. In this study, UV-Vis spectroscopy was utilized, where UV-

Vis refers to ultraviolet-visible wavelength range used for the measurement. In the UV and visible regions of electromagnetic spectrum, atoms and molecules undergo electronic transitions, which means that the energy from UV or visible light is absorbed by a molecule. In such process, one of the electrons jumps from a lower energy to a higher energy molecular orbital. Absorption spectroscopy, in turn, measures such transitions from the ground state to the excited state. A light absorbing molecule is conventionally termed chromophore, which is usually a π-bond containing molecular group, which can be intrinsically present or it can be extrinsically added to the biomolecule via conjugation. Biliverdin, which is a chromophore of studied phytochrome, absorbs light when energy of the photon matches the difference between two energy states of the chromophore molecule. Therefore, UV-Vis absorption spectroscopy is used in this research work to study photocycle of the phytochrome containing biliverdin molecule.

1.6. Unanswered questions and motivation

Despite the extensive research of phytochromes, along with well-established approaches such as NMR, X-ray crystallography, spectroscopic techniques and site-selective mutations, some questions remain unanswered. Things still to be uncovered include the exact structure of photoactivated state and conformational changes happening in photosensory domain of phytochromes which lead to signalling process. Even more exciting is the question of whether we could possibly control the functions of photoreceptors, once we have complete understanding of their functioning mechanisms. By controlling cells with light, it is possible to achieve new breakthroughs in biological research and in medical applications, such as phototherapy or molecular diagnostics. Thus, there is a clear demand to investigate the photochemistry of phytochromes in greater detail.

2. AIMS OF THE STUDY

The main goal of this study is to investigate the switching and photoreversibility of the phytochrome photosensory region *Dr*CBD-PHY between Pr and Pfr states and determine the intermediates of the photoreaction, using UV–Vis spectroscopy and stabilizing intermediates at low temperatures. The focus is placed on the first two intermediates of the forward reaction, namely Pr → Lumi-R and Lumi-R → Meta-Ra transitions (Figure 2). It also seems interesting to determine the maximum yield of the reaction in a reversible state.

Another stream of research is devoted to the investigation of the effect of Serine272 on the stability of Pr state of bacteriophytochrome. There are some evidences that Serine272 may influence water content and interact with the C-ring of chromophore. To check this hypothesis, S272A mutation in *Dr*CBD-PHY was performed (Serine was replaced with Alanine). This mutation served as a tool to figure out whether the mutant will switch between active and inactive states in the same way as the wild type *Dr*CBD-PHY or whether some deviations will be present.

3. MATERIALS AND METHODS

3.1. Bacterial transformation of *Dr*CBD-PHY wild type and mutants

Newly cloned phytochromes were produced in the expression system pET21, using *Escherichia coli* strain BL21DE3. Mutagenesis was previously executed by Heikki Takala. This procedure was done using protocol of QuickChange lightning multi-site-directed mutagenesis kit. Clones contained mutations in the 272nd amino acid where Serine was replaced with Alanine and Cysteine, respectively. Such mutation was chosen due to the hypothesis that Ser272 may interact with the C-ring of biliverdin molecule, as well as may influence water content in that region. CDH5α cells were used for the mutagenized plasmids uptake, whereas B21DE3 cells were utilized for the protein expression. To purify the replicated plasmids inside *E. coli*, only bacterial cells that acquired the plasmid had to be selected. For this purpose, antibiotic resistance selection was performed. EV1 cDNA plasmid contained ampicillin resistance gene, coding for an enzyme beta-lactamase responsible for degrading ampicillin, and was used as a vector to be inserted into competent *E. coli* DH5α. Thus, only bacteria that have acquired the plasmid could grow and divide on the Luria Bertani (LB) growth medium.

Besides the transformation itself, positive and negative controls (have been accomplished. Positive controls enabled to test whether bacteria can grow in normal conditions, whereas negative ones helped to test the efficiency of antibiotic. Thus, four different samples were prepared, among which two samples contained plasmids encoding S272C and S272A mutants, one positive control with original template and one negative control with no template. Amount of plasmid added was 25 ng in each case (except the negative control) per 50 µl of competent cells. To enforce the process of plasmid DNA uptake, all samples were exposed to the heat shock at 42°C for 90 seconds after being incubated on ice for 30 minutes. After this procedure, samples were immediately put on ice for couple of minutes.

800 µl of LB medium were added to each sample which were further incubated at 37°C for 45 minutes shaking at 200 rpm in shaker. During this time, antibiotic resistance genes were expressed and cells recovered after the heat shock. 200 µl of each sample were plated onto appropriate selective LB plate with 100 µg/ml ampicillin. Plates were stored at room temperature until the liquid has been absorbed. The colonies have been left grow at 37°C overnight (approximately 16 hours).

3.2. Protein expression

Two mutants and a wild type phytochrome were expressed and purified according to the same procedure. To prepare the starter culture, a single colony of BL21DE3 glycerol stock of each mutant (S272A and S272C) was taken from transformation plate with grown plasmids, and mixed with 5 ml of LB-medium, containing 5µl (1 µl/ml from stock. 150 mg/ml) ampicillin. The culture was then left to grown in a shaker at 37°C, 200 rpm overnight. All in all, 3x5ml starter culture were prepared (S272A big and small colony as well as S272C mutants).

500 ml of LB medium were added into six 2L Erlenmeyers. 1 ml of starter culture was added to 500 ml of LB-medium along with 500µl (1 µl/ml) of ampicillin to prepare the main culture. It was then incubated at 33°C, 230 rpm for approximately 2 hours. Then the OD_{550} was first measured to check the stage of cultured cell population. When OD_{550} reached 0.5 the SDS-PAGE samples were taken from each main culture. When OD_{550} reached value between 0.5 and 0.65 for both mutants, 500 µl of 1M IPTG (isopropyl β-D-1-thiogalactopyranoside) was added to the main culture to start the induction of proteins. Addition of IPTG to a growing culture of the lysogen induced T7 RNA polymerase production, which in turn transcribed the target DNA in the plasmid. To produce enough proteins, main culture was left at 28°C, 230 rpm overnight.

SDS-PAGE samples were taken from the main culture (from each mutant) before and after the induction. All SDS-PAGE samples were spinned down with Biofuge PICO, Heraeus for 5 min at 5000 rpm at room temperature and pellet was then resuspended in 30 µl of buffer. Afterwards, 30 µl of 2x SDS-PAGE sample buffer were added and the samples were stored in the freezer until the electrophoresis.

To collect the cells, main culture was centrifuged with Sorvall RC 6+ Centrifuge, Thermo Scientific at 4°C, 6000 rpm for 15 minutes. The pellet was suspended with 15 ml of buffer containing 20 mM Tris pH 8.0, 50 mM NaCl, whereupon the supernatant was removed. The suspensions were then transferred into three 50 ml tubes, which were stored at -80 °C until proceeding to purification.

3.3. Protein purification

To collect the proteins, bacterial cell walls were disrupted by applying high pressure in Emulsiflex-C2 homogenizer. The lysate was then cleared from cell debris by certificating with Sorvall Instruments RC5C with Sorvall SS-34 (Du Pont) rotor at 4°C, 25 000 rpm for

30 minutes. In such way, heavier fractions like cell walls and other organelles were separated from all bacterial proteins and DNA molecules. Supernatant was collected and SDS-PAGE samples were taken from pellet and from supernatant. Samples were diluted to 0.5 volume of 2x sample buffer, whereas samples from the pellets were resuspended to 20 mM Tris pH 8.0, 50 mM NaCl and then diluted to 0.5 volume of 2x sample buffer.

At this stage biliverdin has been added to the lysate. Biliverdin was dissolved in the buffer with small amount of 10 M NaOH (900 µl buffer + 100 µl NaOH), the final concentration of biliverdin was 10 mg/50 ml of supernatant. The mixture was incubated on ice and stored in the dark in the cold room overnight.

3.3.1. Affinity chromatography

To achieve high purity of expressed proteins, two phases of purification have been accomplished. At the first capture step of purification, initial purification of the protein was preformed removing the most critical contaminants. On this step, it was critical to rapidly isolate, stabilize and concentrate the protein of interest. Thus, CBD-PHY S272A was separated by affinity chromatography by using Äkta prime (Amersham Pharmacia Biotech) with PrimeView 5.0 program (Amersham Biosciences) using HisTrap FF Crude column, where biochemical properties of the protein were utilized to isolate it from other proteins. The DNA sequence specifying a string of histidine residues, used in vector for production of recombinant proteins with poly-His tag fused to its N- or C-terminus, made it possible for expressed His-tagged proteins to be purified easily, because the string of histidine residues binds nickel resin, while other bacterial proteins did not and hence get discarded.

Studied protein was loaded in the column in sets at the flow rate of 2ml/min with the maximum pressure of 0.5 MPa. The binding buffer consisted of 20 mM Tris, pH 8.0, 50 mM NaCl, 5 mM Imidazole. Eluted proteins were collected in 2 ml fractions with the help of elution buffer containing 20 mM Tris, pH 8.0, 50mM NaCl, 500 mM Imidazole. The gradient was set from 0-100 % (length 50 ml) at 2 ml/min flow rate. After the run, fractions that contained protein based on the chromatogram and appropriate colour (due to the presence of biliverdin) were collected, diluted in SEC buffer, containing 30 mM Tris, pH 8.0 and stored for further purification. Detection wavelength was set to 405 nm. Between the runs, the column was rebalanced with 5x column volumes of elution buffer and binding buffer. SDS-PAGE samples from the pools were collected at the end of this process. These samples were first diluted with 30 mM Tris at pH 8.0 depending on the concentrations and

then 2x sample buffer was added.

The final concentration was measured with Nanodrop spectrophotometer. As the sample volume in SEC was 5 ml per run and the maximum amount of protein was 80 mg per run, the pools were concentrated to needed volume by using Amicon® Ultra-15 10K Centrifugal filters in Megafuge 1.0R (Heraeus) with BS4402/A rotor at 4800 rpm at +4 °C for 10 minutes in the dark. Concentrated protein solution was stored in dark on ice overnight.

3.3.2. Preparative size exclusion

In the intermediate and polishing purification phases the main goal is to separate the target protein from other proteins. Speed is less critical during these phases since the impurities causing proteolysis or other destructive effects should have been removed and sample volume should have been reduced in the capture step. Thus, preparative size exclusion via Äkta Prime liquid chromatography system with the Superdex 75 column was used in the polishing phase of our experiment to achieve high resolution and determine the oligomeric status of studied protein. All mentioned purification steps were conducted in the dark.

Superdex 75 column was equilibrated with SEC buffer overnight. The sample solution was filtered using 25 mm syringe filter with width of 0.45 µm. Protein samples were injected to the column at 2 ml/min flow rate, the maximum pressure was 0.5 MPa. After 6 ml flow, the flow rate was set to 2.5 ml/min. 2 ml fractions that contained protein based on the chromatogram and appropriate colour (due to the presence of biliverdin) were collected on ice.

SDS-PAGE samples were taken from the pools and the concentration was measured with Nanodrop spectrophotometer. Purified protein solution was concentrated to the volume of 3 ml with final concentration of 26.5 mg/ml. Protein solution was aliquoted into 200 µl, 100 µl, 50 µl and 20 µl patches into light safe tubes which have been flash frozen with liquid nitrogen and stored at -80 °C.

3.4. SDS-PAGE

12% SDS-PAGE running and 4% stacking gels were prepared. Before the run, all the samples, except those taken from the chromatograms, were heated at +95 °C for 5 minutes, loaded and run with BioRad cell at 200V for 60 minutes. Gel was stained for 15 minutes, afterwards destaining solution was added and kept overnight. Obtained results were used for analysing the size and concentration of the protein, as well as amount the impurities from

studied samples. Pictures of gel were taking with Bio-Rad detecting equipment. Finally, the absorption of purified protein was measured with NanoDrop-1000 spectrophotometer and concentration of the protein was calculated using Beer - Lambert's law.

3.5. UV-Vis spectroscopy at room and low temperatures

Absorption spectra of both, wild type and the mutant, were measured with the help of Perkin Elmer Lambda 850 UV-Vis spectrophotometer with following settings: scanning was performed in the range from 250 nm to 800 nm with 1 nm data interval and the tungsten lump was selected. To be able to perform spectroscopic measurements, concentrated protein was diluted so that absorbance at 700 nm was approximately 0.3. Polymer cuvettes with 1 cm pathlength were used. Both phytochromes, the wild type and the mutant, were illuminated for 5 minutes with 785 nm light-emitting diode light (LED) to bring them into the inactive state and with 655 nm LED — to get them into the active state. This procedure was repeated couple of times to get more accurate averaged spectra.

Next, the photoreaction of both the forward Pr-Pfr pathway and the backward Pfr-Pr pathway of the wild type phytochrome were investigated at low temperatures, ranging from 80K to the room temperature with 20K intervals. Low temperature was necessary in this experiment due to the short lifetime of some intermediates of the photoreactions. Thus, the main purpose of these measurements was to determine the temperature needed for stabilization of the intermediates. Due to the shorter measuring time, as compared to FTIR spectroscopy, UV–Vis spectroscopy was better suited for this experiment. Measurements were performed in the home-built setup, consisting of Perkin Elmer Lambda 850 UV-Vis spectrophotometer, Oxford Optistat DN cryostat and two LEDs.

To achieve needed low temperatures, Oxford Optistat DN cryostat was assembled and put into the UV-Vis spectrophotometer chamber. Liquid nitrogen was added to reach the lowest possible temperature of 80K and, consecutively heated with 20K intervals using heater. Before measurements, the cryostat was pumped with oil and diffusion pumps to achieve needed pressure of approximately $10^{-9}\,\frac{mbar \cdot l}{s}$. With the oil pump, it was possible to get pressure of $10^{-2}\,\frac{mbar \cdot l}{s}$, whereas to reach needed vacuum diffusion pump was turned on for approximately 30 minutes.

Studied sample was diluted in special buffer which contained SEC buffer (30 mM Tris, pH 8.0) and 66% of glycerol. Glycerol was added to retain photoreversibility of

phytochrome at low temperatures (Foerstendorf 1996). To be able to perform spectroscopic measurements, studied sample was prepared by mixing 3 ml of SEC buffer with 6 ml of 100% glycerol and 20 µl of filtered *Dr*CBD-PHY concentration of 32.48 mg/ml.

Illumination proceeded as following. At first reference measurement was done (the cuvette contained only buffer) to "autozero" the level. Then the phytochrome was switched back and forth between the Pr and Pfr states with the help of 785 nm (far-red, 9-milliwat output power) and 655 nm (red, 7-milliwatt output power) LEDs respectively. At first, phytochrome was illuminated with 785 nm LED for 5 minutes at room temperature (to bring it into the resting state) and the spectrum was taken. Then the laser was switched to 655 nm LED for another 5 minutes to bring phytochrome into the active state and again the spectrum was recorded. The switching procedure was repeated for couple of times to obtain more reliable and accurate difference spectra. Then the cooling was initiated to reach the minimal possible temperature of 80K using liquid nitrogen. During the last measurement at room temperature, the phytochrome was switched into the Pr state and cooled in this state. The same switching procedure of the phytochrome was repeated under 80K, after which the temperature has been increasing with 20K intervals until the room temperature. Spectra of active and inactive states were taken at every temperature level (80K, 100K, 120K, 150K, 160K, 180K, 200K, 220K, 240K, 260K, 280K and RT). It is worth to mention, that the LEDs were switched off during the measurement itself, as well as during the temperature changes.

To determine the maximum yield of the reaction in a reversible state, the same sample was firstly illuminated with 785 nm LED for 15 minutes to bring in into the Pr state. The setup was then cooled with liquid nitrogen down to 180K, after which the series of sequential 655 nm LED illumination and spectra detection started. The spectra were recorded after each 5 minutes of illumination, which brought phytochrome into its active state, for 45 minutes in total. Then the sample was brought back into its inactive state with sequential 5 minutes' illuminations with 785 nm LED for 20 minutes in total. From this set of measurements, it was possible to construct difference spectra of interest to observe increase of the photoreaction, as well as return to its initial state.

4. RESULTS

4.1. CBD-PHY mutants were successfully expressed and purified

After the overnight incubation, the transformation plate with samples having plasmids encoding S272C and S272A mutants contained some bacterial colonies (approximated to ~ 200-250 colonies). The negative control plate was totally empty and the positive control plate was full of colonies (~thousands). Thus, there were much more colonies on positive control plate than on the experimental plate. It was interesting that mutant S272A produced different types of colonies: the most colonies were of similar size, whereas there was one unusually small colony. Both colonies were considered for further protein expression.

The gels from production and purification of the mutant S272A are shown in Figure 3. Both mutants S272A and S272C were successfully expressed except for the small colony of S272A, which is presumably because the small colony itself was defective. Only the mutant S272A was considered for the purification steps. After the induction of IPTG, a clear increase in both mutants' production can be seen in the gel at around 57 kDa.

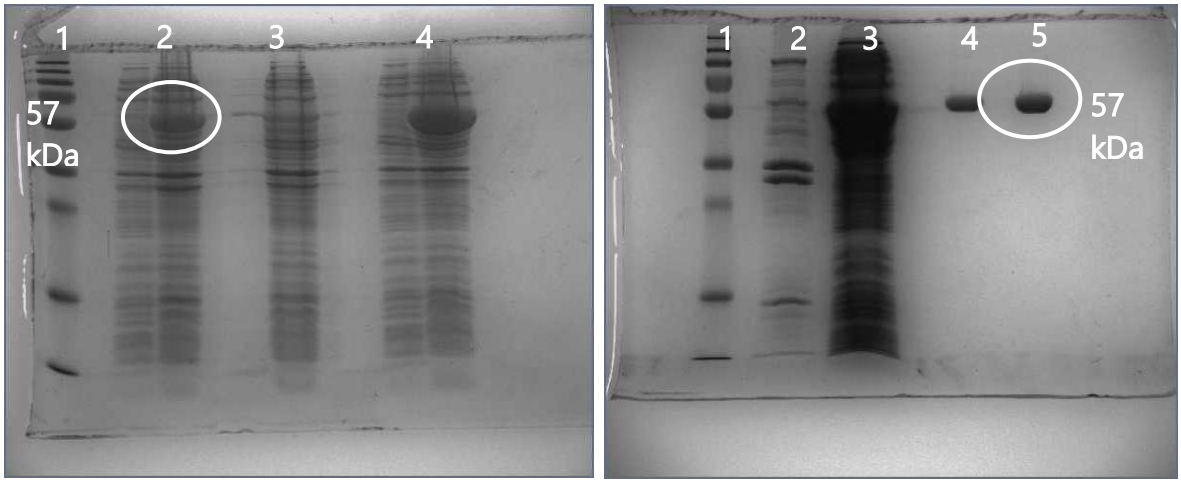

Figure 3: **Production and purification of the CBD-PHY mutants**. Left part: SDS-PAGE gel from different samples, namely sample 1 - molecular standard, sample 2 - S272A bigger colony, sample 3 - S272A smaller colony, sample 4 - S272C, the uninduced samples are shown in the right column, and induced – in the left column. Right part presents the lysis and chromatography samples, namely sample 1- molecular standard, sample 2 - bacterial pellet, 3 - bacterial lysate, 4 - HIS purification, 5 - SEC purification

After the cell lysis process, it can be clearly seen that sample with bacterial pellet contains only small amount of the mutant of interest (Figure 3, right part, sample 2). Whereas presence of large amount of S272A can be distinguished in the supernatant sample. Both steps of the purification proceeded successfully, the protein with the size of around 57kDa can be observed in the purification part of the gel, meaning that *Dr*CBD-PHY

fragments were purified and no other fragments of the phytochrome were present in the final pool.

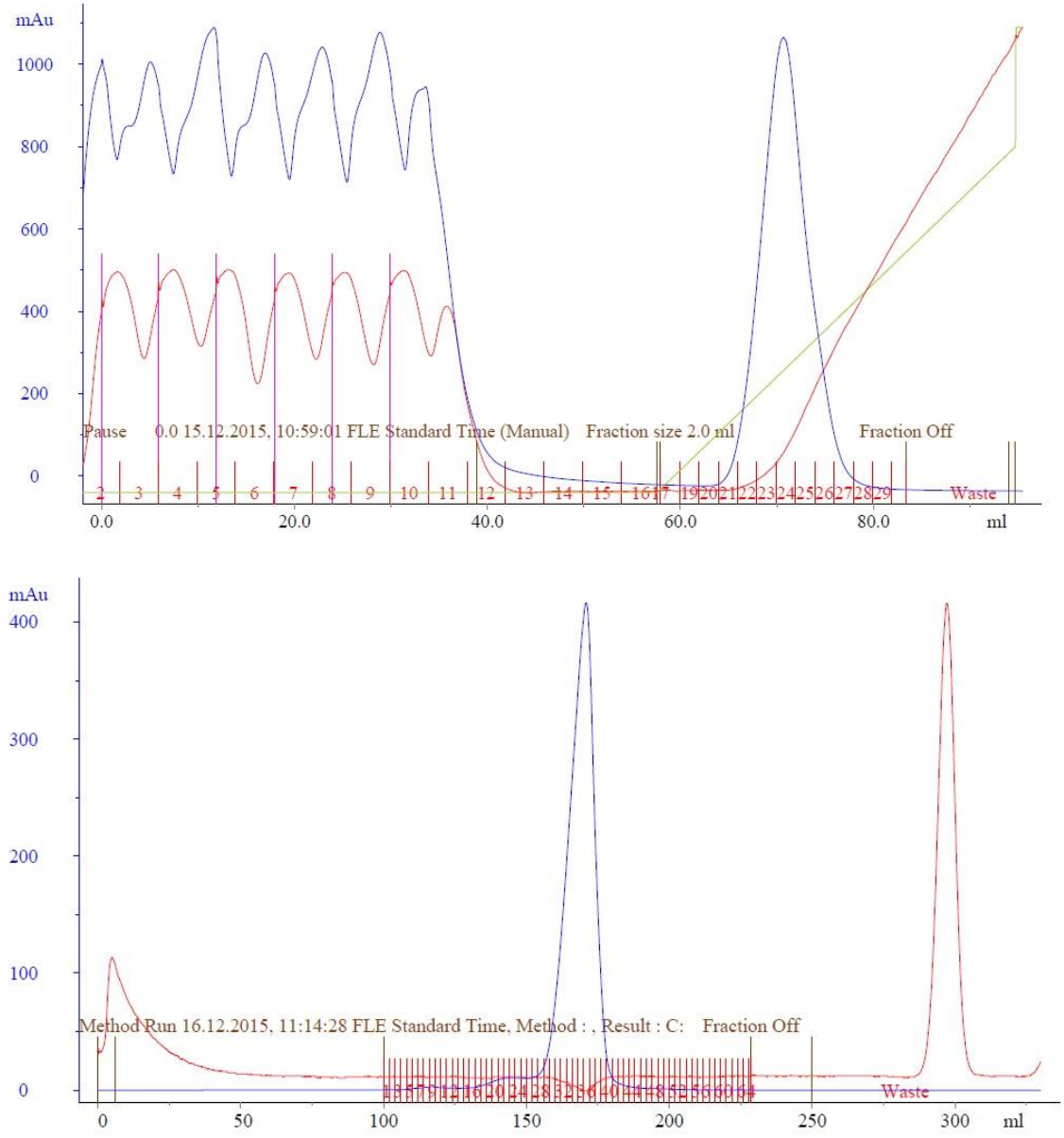

Figure 4: **Purification of CBD-PHY S272A via affinity chromatography and size-exclusion chromatography.** Chromatograms from affinity and preparative size-exclusion chromatography are shown in upper and lower parts, respectively. Blue line represents absorbance, red line - conductivity red and green line - concentration of the elution buffer. Detection wavelength was set to 405 nm, both in affinity and SEC.

During the first step of purification of *Dr*CBD-PHY S272A mutant (affinity chromatography) samples were injected to the column in several sets (Figure 4, upper part). These injections correspond to absorbance and conductivity peaks between 0-50 ml on the chromatogram, where blue and red represent absorbance and conductivity, respectively.

The phytochromes of interest started to elute after the concentration of the elution buffer reached 20 %, which corresponds to about 100 mM concentration of imidazole. To proceed for the next purification step, the protein was concentrated to 15.075 mg/ml and the amount of protein solution was 10 ml.

Preparative SEC with high resolution column was performed to understand the oligomeric status of the purified mutant (Figure 4, lower part). On the SEC chromatogram, the small volume of the larger fragment eluted at 150 ml can be seen. This fragment could possibly be a formed dimer in the process of the expression. The size of the *Dr*CBD-PHY dimer is approximately 90 kDa, thus the main peak at 170 ml corresponds to monomeric *Dr*CBD-PHY S272A, which weights around 57 kDa. The concentration of the studied phytochrome after the final step of purification was 26.5 mg/ml. Overall, the amount and purity of the expressed mutants was similar to the wild type.

4.2. Absorption spectra at room temperature provide comparison between the switching of the wild type phytochrome and its S272A mutant

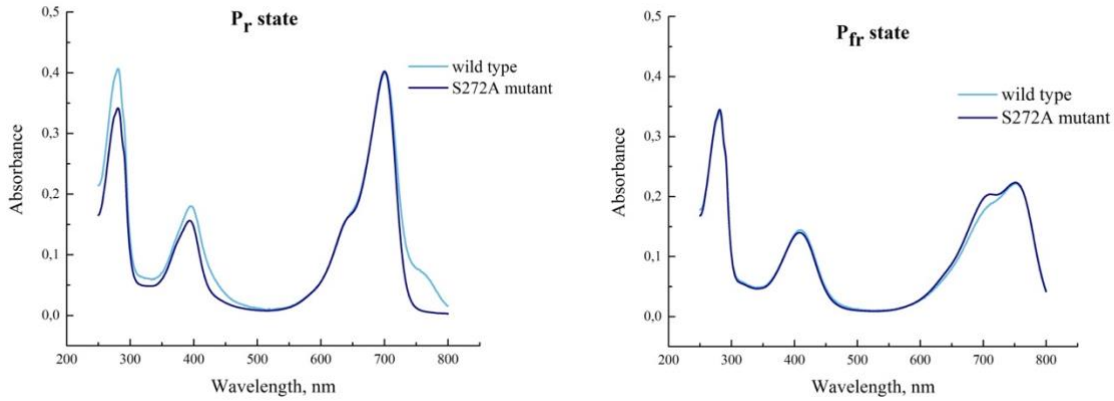

Figure 5: **Absorption spectra of *Dr*CBD-PHY wild type and S272A mutant in active and inactive state.** Left part: Pr state absorption spectra of wild type and S272A show similar pattern with the same absorption maxima at 655 nm and 400 nm corresponding to first and second excitation states of biliverdin, respectively. Right part: Pfr state absorption spectra of wild type and S272A mutant with absorption maxima at 785 nm and 400 nm corresponding to first and second excitation states of biliverdin, respectively.

Chromophore biliverdin strongly absorbs light around 700 nm. Absorbing a photon with wavelength $\lambda \sim 700$ nm, the molecule transits into its first excited state, and absorbing a photon with $\lambda \sim 400$ nm — into its second excited state. Absorption spectra of protein fragments after illumination with far-red (785 nm) and red (655 nm) light, labelled Pr and Pfr respectively are represented in the Figure 5. Absorption spectrum of the Pr state also shows that absorbance at 700 nm (first excited state of biliverdin) is stronger than at 400 nm

(second excited state of biliverdin).

Absorbance peak at around 280 nm represents absorbance of the phytochrome protein itself. Aromatic amino acids tryptophan, tyrosine and phenylalanine are responsible for most of the absorbance of ultraviolet light, they absorb at 280 nm, 274 nm and 257 nm, respectively.

The main goal of the mutation was to identify the effect of Serine272 on the stability of the photocycle. This mutation served as a tool to figure out whether the mutant will be able to switch between active and inactive states in the same way as the wild type *Dr*CBD-PHY. In other words, it was interesting to check whether Serine272 is essential for the photoreaction stability. Absorption spectra from the Figure 5 clearly show that S272A mutant adopts both Pr and Pfr states, meaning that it is capable of reversible photoswitching process. However, despite the similar behaviour, spectra of the mutant and wild type are different (dark- and light- blue spectra, respectively). For instance, there is less of Pr state in mutant than in the wild type (Figure 5, left). Moreover, in the Pfr state the absorption spectrum of the mutant has more pronounced shoulder at approximately 700 nm, as compared to the wild type (Figure 5, right).

At this stage of the experiment, it became clear that Serine272 does not really influence the stability of the photocycle, as well as the photoreversibility of the process. Thus, further steps of this work, namely the UV-Vis spectroscopy at low temperatures, only investigate *Dr*CBD-PHY wild type.

4.3. UV-Vis spectroscopy reveals stabilized intermediates of the *Dr*CBD-PHY photocycle at low temperatures

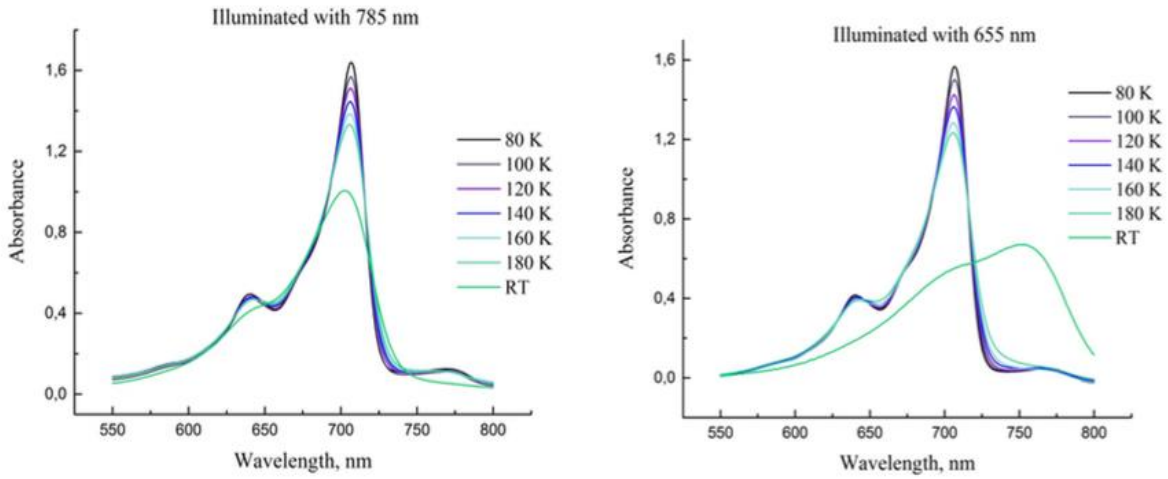

Figure 6: **UV-Vis absorption spectra of *Dr*CBD-PHY under illumination at 785 nm and 655 nm at different temperatures.** Left part: absorption spectra of *Dr*CBD-PHY under 785 nm illumination at temperatures ranging from 80K up to room temperature. Right part: absorption spectra of *Dr*CBD-PHY under 655 nm illumination at temperatures ranging from 80K up to room temperature. The difference in the pattern of spectra in the Pfr state as compared to Pr state cannot be really seen at low temperatures, creating a need for more close investigation with the help of difference spectra.

At first it was necessary to determine whether *Dr*CBD-PHY construct can undergo the photoreaction under low temperatures. Thus, Figure 6 represents the absorption spectra at temperatures ranging from 80K to room temperature. All measurements were taken from the same sample, which contained glycerol to retain photoreversibility at low temperatures. The absorbance maxima in Pr and Pfr states at room temperature can be clearly distinguished and observed at around 700 nm and 765 nm, respectively. However, when the temperature drops down to 180K, transition between states becomes less obvious (different behaviour between spectra in both states cannot be clearly distinguished). Thus, it seems reasonable to construct difference spectra to investigate photoswitching of *Dr*CBD-PHY under low temperatures in more detail. Nevertheless, already at this point of the experiment, it is clear that behaviour of spectra at low temperatures is different as compared to the room temperature. Moreover, new band at 780 nm in Pr state arises at low temperatures.

Thus, photoreactions of both the forward Pr-Pfr pathway and the backward Pfr-Pr pathway have been further investigated at low temperatures, ranging from 80K to room temperature, at 20K intervals. From the distinct pattern of the difference spectra, it became reasonable to distinguish three temperature ranges, namely from 80K to 120K, 140K to 180K and 220K to room temperature. The main purpose of these studies was to determine temperature for stabilizing intermediates, as well as their absorption maxima.

UV-Vis difference spectra between Pr and Pfr (forward reaction) and between Pfr and Pr (backward reaction) of *Dr*CBD-PHY at low temperatures in 80 – 120K temperature range are shown in Figure 7. The difference in absorption spectra is very small, meaning that reaction yield is low at such low temperatures. This, in turn, means that phytochrome did not complete switch from one state to another. However, even at 80K observable changes between states exist.

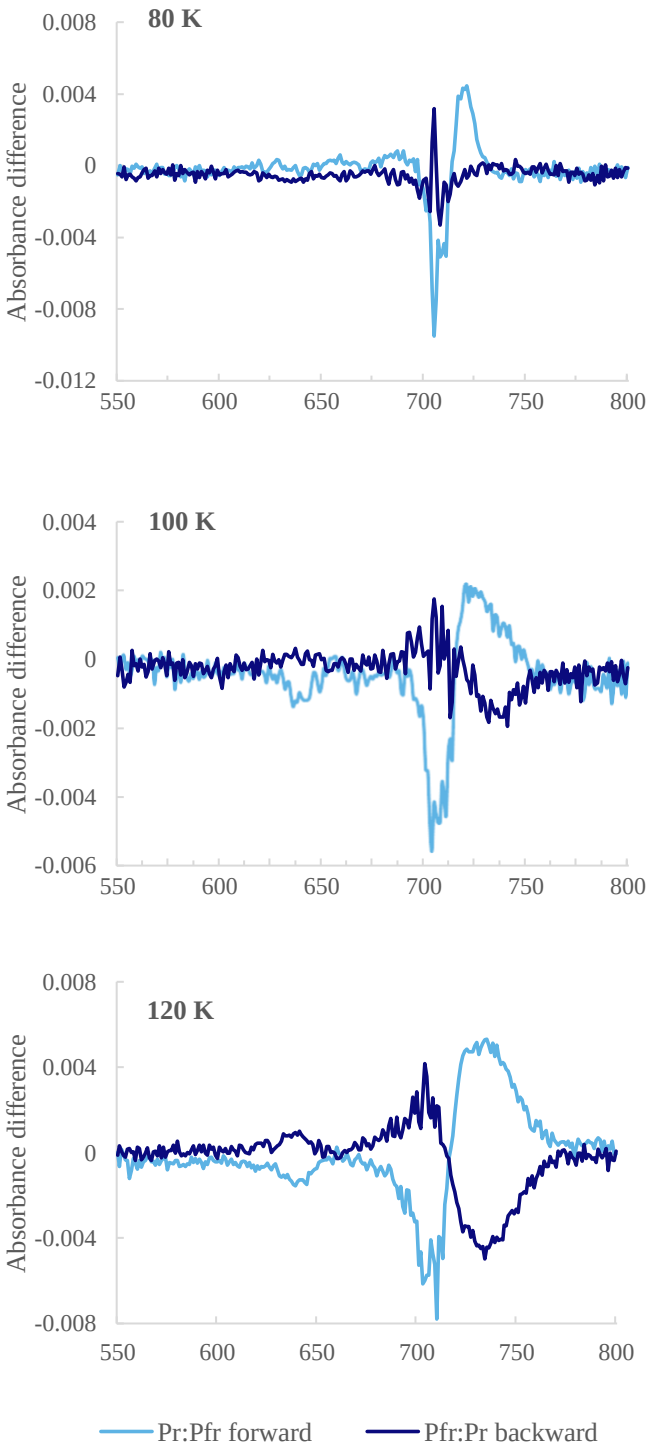

Figure 7: **UV-Vis difference spectra of *Dr*CBD-PHY at low temperatures in 80 – 120K temperature range.** Upper part: difference spectra for forward (Pr-Pfr) and backward (Pfr-Pr) reactions of *Dr*CBD-PHY at 80K. The difference in absorption spectra is very small, meaning that reaction yield is low at such temperatures, which, in turn, means that phytochrome did not complete switch from one state to another. However, even at this level observable changes between states exist. The backward reaction is insignificant, leading to the conclusion that such change is not reversible at 80K utilizing 785 nm LED.

Middle part: difference spectra for forward and backward reactions at 100K. As the temperature increases, the yield of the reactions increases as well, however the backward reaction is still very low, meaning that at this temperature level the process is still not reversible.

Lower part: difference spectra for forward and backward reactions at 120K. The yield of the forward reaction is almost comparable to that at 100K, however, the backward reaction becomes significant at this temperature level and the process becomes reversible. Overall, it is clear from the graphs that reversibility increases with temperature.

The backward at 80K reaction is insignificant, leading to the conclusion that Lumi-R is not reversible with the 785 nm LED. As the temperature increases to 100K, the yield of the reactions increases as well, however the backward reaction is still very low. At 120K, the yield of the forward reaction is almost comparable to that at 100K, however, the backward reaction becomes significant at this temperature level and the process becomes reversible.

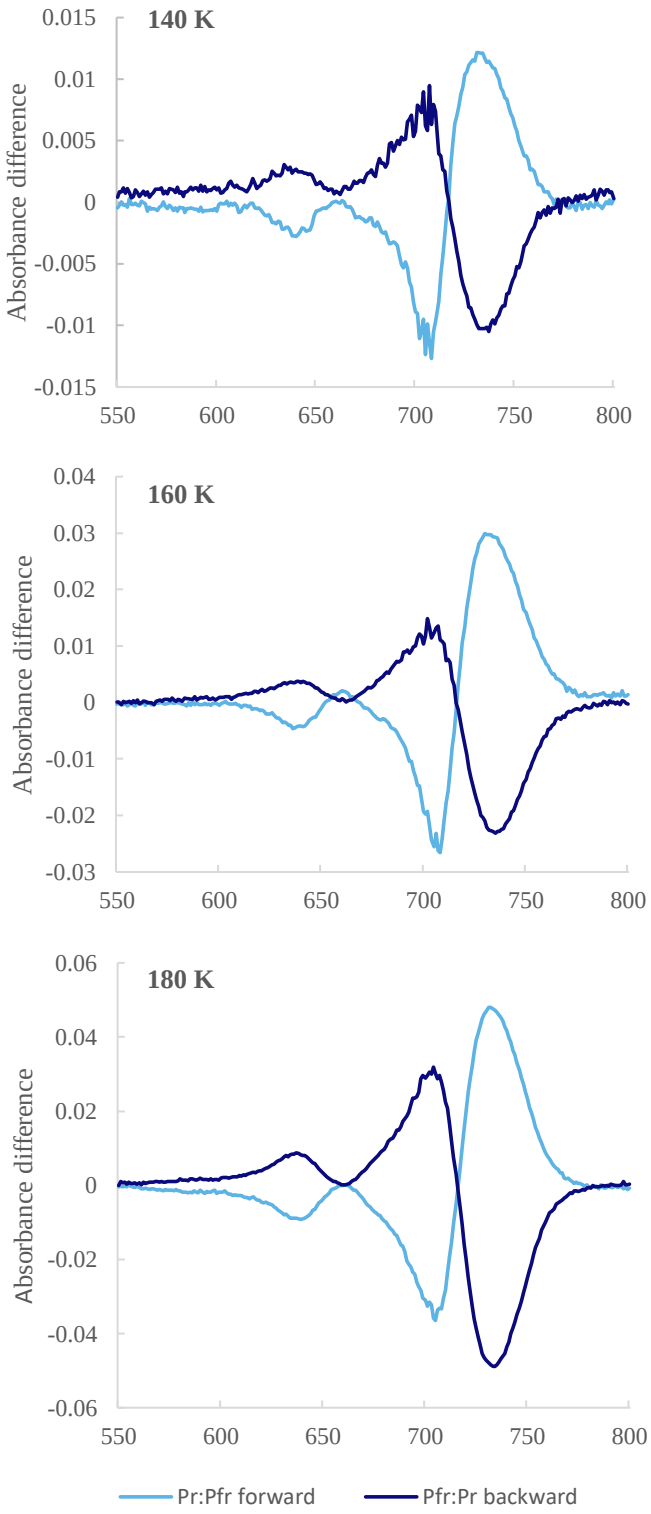

Figure 8: **UV-Vis difference spectra of *Dr*CBD-PHY at low temperatures in 140 – 180K temperature range. First evidences of photoreversibility.**

Upper part: difference spectra for forward (Pf-Pfr) and backward (Pfr-Pr) reactions at 140K. Difference spectra of both reactions have increased as compared to the previous temperature level, indicating that greater number of proteins were able to switch from one state to another.

Middle part: difference spectra for forward and backward reactions at 160K. Yield of both reactions has almost doubled as compared to the previous temperature level.

Lower part: difference spectra for forward and backward reactions at 180K. Again, difference spectra almost doubled as compared to the previous temperature level. As the yield of backward reaction has reached that of the forward one (moreover it became even larger), conclusion to make here is that changes between resting and active states have become completely reversible.

Overall, it is clear from the graphs that yield of the photoreaction, as well as reversibility of the process increases with temperature, and thus intensity of the difference band increases from about 2 mOD at 80K (Figure 7) to about 40 mOD at 180K (Figure 8, lower part). Intensity of both, Pr-Pfr and Pfr-Pr difference spectra strongly depends on the temperature, which disagrees with other findings (Schwinte 2009).

UV-Vis difference spectra of *Dr*CBD-PHY at the temperature range of 140 – 180K are shown in Figure 8. Upper part of the figure (140K) shows that yields of both reactions have increased as compared to the previous temperature range, indicating that greater number of proteins were able to switch from one state to another. At the temperature level of 160K, the yield of both reactions has almost doubled as compared to the previous temperature level. At 180K difference spectra almost doubled again as compared to the previous temperature level. As the yield of backward reaction has reached that of the forward one (moreover it became even larger), meaning that changes between resting and active states have become completely reversible. Another interesting observation to mention here is that forward and backward reactions lack the mirror image in all temperature ranges shown until now.

UV-Vis difference spectra from forward reaction in all temperature ranges are shown in Figure 9. At 80K, 100K and 120K the pattern of the spectra is clearly distinct from all other spectra at more higher temperatures. The magnitude of the difference spectra of the reactions is very small in this temperature range. Clear increase of the yield of reaction as the temperature rises is observable: yield of the forward reaction at 80K-120K is very small (6 mOD), at 140K-180K it increases by approximately one order of magnitude (40 mOD), at the level of 230K it increases dramatically, resembling the room temperature case (200 mOD).

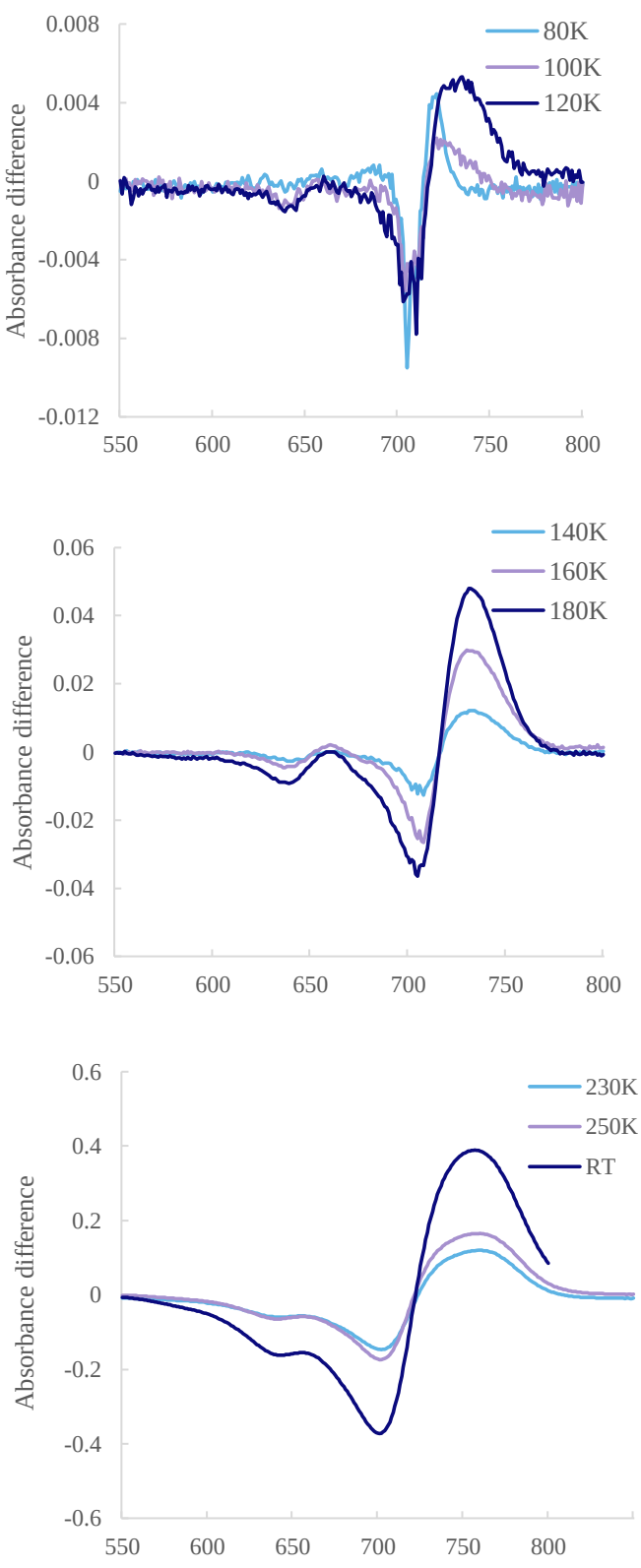

Figure 9: **UV-Vis difference spectra of *Dr*CBD-PHY at all temperature ranges with only forward reaction shown.**

Upper part: UV-Vis difference spectra *Dr*CBD-PHY at 80K, 100K and 120K. Here the forward reaction is shown. The magnitude of the difference spectra of the reactions at the temperature range of 80K-120K is very small.

Middle part: UV-Vis difference spectra *Dr*CBD-PHY at 140K, 160K and 180K. Here the forward reaction is shown. Again, the clear increase of the reaction's yield is observable.

Lower part: UV-Vis difference spectra *Dr*CBD-PHY at 230K, 250K and room temperature. Here the forward reaction is shown. At these temperatures forward reaction resembles the room temperature case.

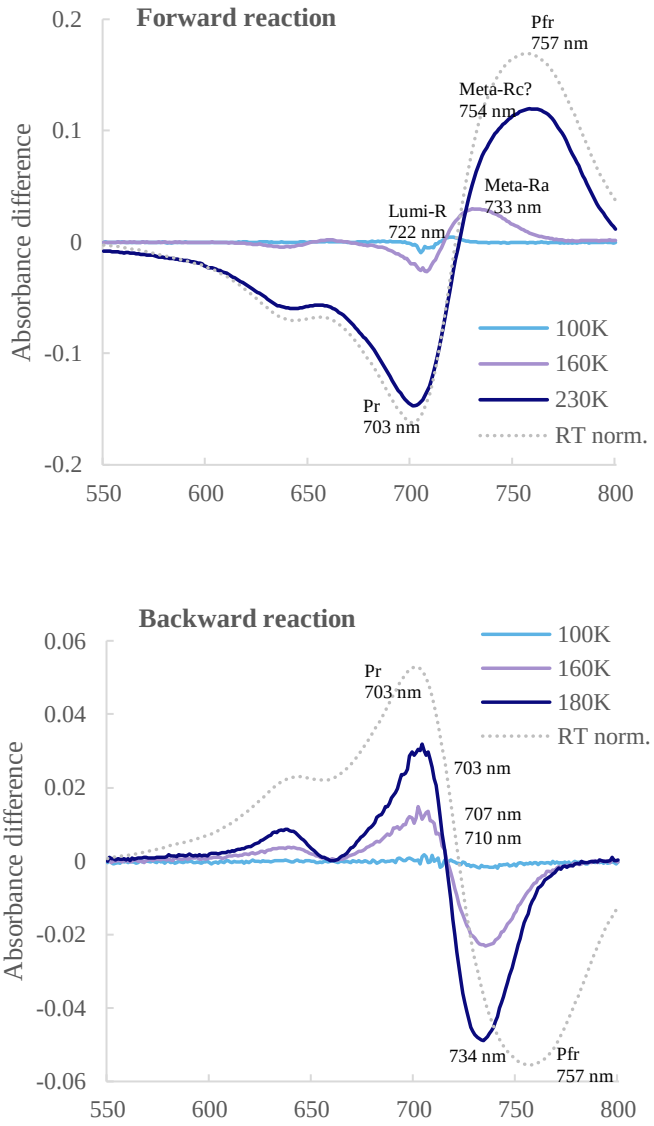

Figure 10: ***Dr*CDB-PHY difference spectra of forward and backward reactions from each temperature ranges.**

Upper part: One of the difference spectra from each temperature range and the normalized room temperature spectrum of the forward reaction are shown here. Distinct behavior of difference spectra inherent to different temperature rages may presumably indicate presence of at least two different intermediates of the photoreaction. Detected maxima at 722 nm (Lumi-R), 733 nm (Meta-Ra), 754 nm (presumably Meta-Rc) and 757 nm (Pfr), detected minima at approximately 703 nm for all temperatures.

Lower part: One of the difference spectra from each temperature range (except for the third one) and the normalized room temperature spectrum of the backward reaction is shown here. Detected maxima at 703 nm, 707 nm and 703 nm, at detected minima at approximately 734 nm and minimum for RT case – at 757 nm.

*Dr*CDB-PHY difference spectra of forward reaction from each temperature range are presented in Figure 10. These graphs show one difference spectrum from each temperature range as it has been discussed earlier. It can be clearly seen, that the difference spectrum becomes broader as the temperature increases. Such broadening means shift of the absorption maxima for both reactions, however this effect is stronger pronounced in the forward reaction case. Distinct behaviour of difference spectra inherent to different temperature rages presumably indicates presence of three different intermediates of the photoreaction. Namely, Lumi-R can be only obtained at temperatures lower then 120K and its corresponding absorption maximum is at 722 nm. Meta-Ra intermediate can be seen in a temperature range of 140K – 180K with absorption maximum at 733 nm. Presumably, Meta-Rc intermediate can be distinguished starting from 220K, its absorption maximum is at 754 nm. However, behaviour of the difference spectrum at this temperature level closely resembles that of the room temperature case (absorption

maximum at 757 nm), which impugns presence of Meta-Rc state at all. It is possible that two intermediates – Meta-Ra and Meta-Rc form one single intermediate Meta-R during the photoreaction. In case of backward reaction, there is smaller shift of the maximum at 733 nm (at 100K) to 735 nm (at 180K) and finally to 757 nm in the room temperature case. It is possible, that these small shift of the maximum indicate presence of yet another two different intermediates, which are between Pfr and some forward reaction intermediates.

4.4. UV-Vis measurements made it possible to observe maximum yield of the forward reaction of *Dr*CBD-PHY and gradual return to its original state

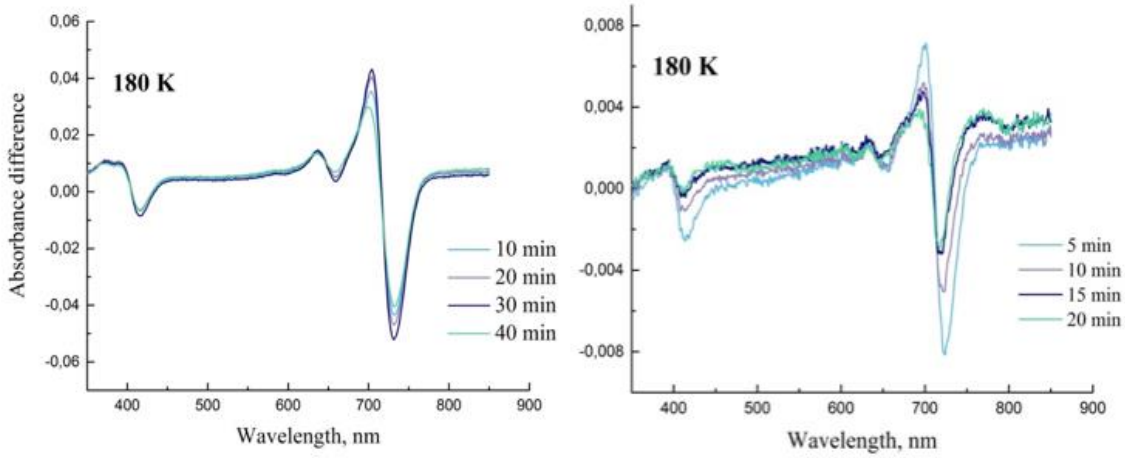

Figure 11**: Maximum yield of the forward reaction and gradual return to original state at 180K**

Maximum yield of the forward photoreaction and its gradual return to original state at 180K is shown in Figure 11. This particular temperature was selected due to the previous finding, namely that at 180K changes between resting and active states have become completely reversible. Initially the sample was brought into the Pr state with the help of 785 nm LED illumination. Then, series of sequential 655 nm LED illumination and spectra detection started. Difference spectra constructed after each illumination series can be seen in the left part of the Figure 11. Then, the sample was brought back into its inactive state with sequential 5 minutes' illuminations with 785 nm LED for 20 minutes in total (Figure 11, right part). Thus, forward reaction yield increases with time, whereas backward reaction gradually returns to the original state and already after 20 minutes, the magnitude of the difference spectrum drops to approximately 2 mOD.

5. DISCUSSION

5.1. Serine272 has no effect on the stability of the photoreaction

Both, production and purification of the mutant S272A went successfully, as expected. Procedures for production and purification were exactly like those applicable for the wild type *Dr*CBD-PHY. During the spectroscopic measurements at the room temperature it appeared clear that absorption spectra of both, the wild type and the mutant, behave similarly: both proteins could switch between Pr and Pfr states of the photoreaction under far-red and red illumination. However, despite the similar behaviour of the spectra, there was less of Pr state in mutant than in the wild type. Moreover, in the Pfr state the absorption spectrum of the mutant had more pronounced shoulder at approximately 700 nm, as compared to the wild type (Figure 5). Nevertheless, we cannot confidently claim that these differences are constant. One possible explanation for existence of such differences could be presence of some light in the sample, meaning that part of the sample had already switched to Pfr state. Thus, conclusion to make here is that Serine272 does not influence the stability of the photocycle, as well as the photoreversibility of the process, as has been speculated previously.

5.2. Stabilized intermediates have been revealed at low temperatures

Pr:Pfr pathway. Different behavior of absorption spectra at various temperature ranges can indicate presence of at least two intermediates of the photoreaction. In the Pr:Pfr photoreaction, only one minimum at approximately 703 nm corresponding to the disappearance of the Pr state was observed. As for the maxima, Lumi-R intermediate has clearly distinct behavior with absorption maximum at 722 nm achievable below 120K. The following intermediate has doubled intensity and its maximum redshifts towards 733 nm. Due to these distinctions from the previous intermediate, we can safely conclude that this is another intermediate, presumably Meta-Ra. Following Meta-Ra, should appear Meta-Rc intermediate, however behavior of its difference spectrum, as well as absorption maximum closely resembles room temperature case and thus is similar to usual Pfr state. Absorption maximum at room temperature lies at 757 nm, whereas obtained data for 230K indicates absorption maximum at 754 nm. Thus, interesting question arises, whether Meta-Ra and Meta-Rc states are distinguishable. It may be the case, that small difference in the absorption maxima of Pfr state obtained at room temperature and that of presumable Meta-Rc state obtained at 230K, is only due to measurement error and in reality, there is no Meta-Rc state

as a separate intermediate. Thus, it appears that there is a Meta-R state, which is a combination of Meta-Ra and Meta-Rc intermediates. Thus, in the temperature range of 140-180K Meta-R state can be trapped. Further increase of temperature becomes difficult, due to sample crystallization. It is almost impossible to reliably measure absorption spectra in the temperature range of 200-220K. Perhaps another sample buffer could solve this issue.

As for the yield of photoreaction, it increases with rising of temperature and therefore the intensity of the difference spectrum increases from about 4mOD at 80K to 400 mOD at the room temperature. Thus, intensity of the Pr:Pfr difference spectra strongly depends on the temperature. Moreover, the difference spectrum becomes broader as the temperature increases.

Pfr:Pr pathway. The intensity of the backward reaction increases with the temperature as in the case of forward reaction. These findings, however, contradict with those found by other researchers for the photoreaction of the chromophore form cyanobacteria (Schwinte 2009). In the same time, there is one minimum at 734 nm for all temperatures (except for the room temperature case) corresponding to the disappearance of the Pfr state (Figure 10, lower part). At the temperature of 100K, maximum is located at 710 nm, which can presumably indicate existence of another intermediate. Maximum is then blueshifted to 707 nm at 160K. Again, this small shift may represent transition to the next intermediate state. The most blueshifted peak is observed at 703 nm in the Pr difference spectrum. Nevertheless, it is not clear, whether these small shifts in the maxima are significant changes or they may be causes by a measurement error. On the other hand, we can observe lack of the mirror image at all temperature ranges (Figures 7 and 8), which is another argument for the presence of different intermediates of the photoreaction.

In both pathways discussed here, the yield of the forward- and backward reactions is temperature-dependent, indicating absence of the barrier-free reaction path.

Useful finding is that intensity of the backward reaction under 80K is so small, that we may speak that there is no backward reaction at all. Thus, it is advisable to use another laser to switch the phytochrome to the desired state.

6. CONCLUSION

Findings of this work do not support hypothesis that stability of the Pr state depends on the presence of Serine272. *Dr*CBD-PHY S272A mutant can be successfully expressed and purified with usual techniques using affinity and preparative size exclusion chromatography. Moreover, experiment showed that S272A mutant indeed can undergo the switching between the two states and the absorption maxima are the same as for the wild type. However, some differences in the pattern of absorption spectrum as compared to the wild type, are present. Overall, these findings mean that Serine272 has no effect on the stability of the photocycle, as well as the photoreversibility of the process.

The photoreaction of both the forward Pr:Pfr pathway and the backward Pfr:Pr pathway was investigated at low temperatures, ranging from 80K to room temperature, at 20K intervals. Reliable difference spectra received with the help of UV-Vis spectroscopy presented in this study, identified intermediates for both pathways of the photoreaction of *Dr*CBD-PHY. Spectroscopy studies revealed that there are observable changes between two sates of the phytochromes already at 100K. There seem to exist three different temperature ranges 80K – 120K, 140K – 180K, 230K – RT, where spectra show distinct behaviour, namely different absorption maxima are inherent to each of the selected temperature range. This fact presumably indicates presence of at least two different intermediates of the forward photoreaction. Moreover, the absence of mirror image in the difference spectra of forward and backward reaction strengthen above mentioned conclusion. Interesting observation is that there are no distinct Meta-Ra and Meta-Rc states, rather there exists one Meta-R intermediate, which presumably is a combination of them. We now can deduce the absorbance maxima in the difference spectra for the stabilized intermediates in the forward photoreaction: the first intermediate (Lumi-R) is only obtained at temperatures lower than 120K and the corresponding absorption maximum in the difference spectrum is estimated to 722 nm. Lumi-R is followed by Meta-R intermediate with absorption maximum at 733 nm. It has been also shown that both, reversibility and yield of the forward and backward photoreactions increase with temperature. As for the backward reaction, identification of the intermediates is less reliable due to insignificant shifts in the absorption maxima. Intermediates of the backward reaction can be achieved at 100K and its absorption maximum is located at 710 nm. Under 160K it is possible to observe another intermediate with its blueshifted maximum at 707 nm.

Thus, from the UV–Vis low temperature investigations we could select a set of optimal temperatures to further study these photoproducts by FTIR difference spectroscopy if needed. These selected temperatures for the Pr:Pfr pathway are:100K and 160K. As the next step of the research, FTIR difference spectroscopy can be used to study the intermediates in more detail.

7. REFERENCES

Andel, F., 3rd, Lagarias, J. C., Mathies, R. A. 1996. *Biochemistry* 35 15997–16008

Andel F., Hasson K.S., Gai F., Anfinrud P.A., Mathies R A. 1997. Femtosecond time-resolved spectroscopy of the primary photochemistry of phytochrome. *Biospectroscopy*. 3(6):421-433

Andel, F., 3rd, Murphy, J. T., Haas, J. A., McDowell, M. T., van der Hoef, I., Lugtenburg, J., Lagarias, J. C., Mathies, R. A. 2000. *Biochemistry* 39 2667–2676

Auldridge, M.E. and K.T. Forest. 2011. Bacterial phytochromes: more than meets the light. *Crit. Rev. Biochem. Mol. Biol.* 46(1):67-88

Bhate M. P., Molnar K. S., Goulian M., DeGrado W. F. 2015. Signal transduction in histidine kinases: Insights from new structures. *Structure* 23, 981–994

Bhoo, S.H., J.S. Davis, J. Walker, B. Karniol and R.D. Vierstra. 2001. Bacteriophytochromes are photochromic histidine kinases using a biliverdin chromophore. Nature. 414:776-779

Bischoff M., Hermann G. 2001. *Biochemistry* 40, 181-186

Björling A., Berntsson O., Takala H., Gallagher K. D., Patel H., Gustavsson E., St. Peter R., Duong P., Nugent A., Zhang F., Berntsen P., Appio R., Rajkovic I., Lehtivuori H., Panman M. R., Hoernke M., Niebling S., Harimoorthy R., Lamparter T., Stojković E. A., Ihalainen J. A., Westenhoff S. 2015. Ubiquitous structural signalling in bacterial phytochromes. J. Phys. Chem. Lett. 6, 3379–3383

Björling A., Berntsson O., Lehtivuori H., Takala H., Hughes A. J., Panman M., Hoernke M., Niebling S., Henry L., Henning R., Kosheleva I., Chukharev V., Tkachenko N., Menzel A., Newby G., Khakhulin D., Wulff M., Ihalainen J., Westenhoff S. 2016. Structural photoactivation of a full-length bacterial phytochrome. Scientific Advances

Borucki, B., von Stetten, D., Seibeck, S., Lamparter, T., Michael, N., Mroginski, M. A., Otto, H., Murgida, D. H., Heyn, M. P., Hildebrandt, P. 2005. J. Biol. Chem. 280 34358–34364

Borucki B., Seibeck S., Heyn M. P., Lamparter T. 2009. Characterization of the covalent and noncovalent adducts of Agp1 phytochrome assembled with biliverdin and phycocyanobilin by circular dichroism and flash photolysis. *Biochemistry* 48, 6305–6317

Burgie, E.S., J. Zhang and R.D. Vierstra. 2016. Crystal structure of Deinococcus phytochrome in the photoactivated state reveals a cascade of structural rearrangements during photoconversion. *Structure*. 24:448-457

Dasgupta J., Frontiera R. R., Taylor K. C., Lagarias J. C., Mathies R. A. 2009. Ultrafast excited-state isomerization in phytochrome revealed by femtosecond stimulated Raman spectroscopy. *Proc. Natl. Acad. Sci. U.S.A.* 106, 1784–1789

Eilfeld, P. and W. Rüdiger. 1985. Absorption spectra of phytochrome intermediates. *Z Naturforsch*. 40c:109-114.

Essen L.O., Mailliet J., Hughes J. 2008.The structure of a complete phytochrome sensory module in the Pr ground state. *Proc. Natl. Acad. Sci. U.S.A.* 105, 14709–14714

Gartner W, Braslavsky S.E. 2003. The phytochromes: spectroscopy and function. *In Photoreceptors*

and Light Signalling, ed. A Batschauer, pp. 136–80. Cambridge, UK: Roy. Soc. Chem.

Kendrick R.E. 1994 *J. Photochem. Photobiol*. B 23, 91

Kneip, C., Hildebrandt, P., Schlamann, W., Braslavsky, S. E., Mark, F., Schaffner, K. 1999. *Biochemistry* 38 15185–15192

Kneip, C., Schlamann, W., Braslavsky, S. E., Hildebrandt, P., Schaffner, K. 2000. *FEBS Lett*. 482252–256

Lamparter, T. 2004. Evolution of cyanobacterial and plant phytochromes. *FEBS Lett*. 573(1-3):1-5

Mizutani, Y., Tokutomi, S., Kitagawa, T. 1994. *Biochemistry* 33 153–158

Mroginski, M. A., Murgida, D. H., von Stetten, D., Kneip, C., Mark, F., Hildebrandt, P. 2004. *J. Am. Chem. Soc*. 126 16734–16735

Mroginski M. A., Murgida D. H., Hildebrandt P.2007. The chromophore structural changes during the photocycle of phytochrome: A combined resonance Raman and quantum chemical approach. *Acc. Chem. Res*. 40, 258–266

Pratt L.H. 1995. *Photochem. Photobiol*. 61, 10

Quail, P.H. 2002. Phytochrome photosensory signalling networks. *Nat Rev Mol Cell Biol*. 3:85-93.

Robben U., Lindner I., Gärtner W. 2008. New open-chain tetrapyrroles as chromophores in the plant photoreceptor phytochrome. *J. Am. Chem. Soc*. 130, 11303–11311

Rockwell, N.C., Y.S. Su and J.C. Lagarias. 2006. Phytochrome structure and signaling mechanisms. *Annu Rev Plant Biol*. 57:837-858

Rockwell, N.C. and J.C. Lagarias. 2006. The structure of phytochrome: a picture is worth a thousand spectra. *Plant Cell*. 18:4-14

Rockwell, N.C. and J.C. Lagarias. 2010. A brief history of phytochromes. *Chemphyschem*. 11(6):1172-1180

Rudiger W., Thummler F. 1991. *Angew. Chem., Int. Ed. Engl*. 30, 1216

Sage L.C. 1992. Pigment of the Imagination: A History of Phytochrome Research. *San Diego: Academic*. 562 pp.

Sineshchekov, V.A. 1995. Photobiophysics and photobiochemistry of the heterogeneous phytochrome system. *BBA-Bioenergetics*. 1228:125-164

Smith, H. 2000. Phytochromes and light signal perception by plants in emerging synthesis. *Nature* 407, 585-591

Spruit C.J.P., Kendrick R.E., Cooke R.J. 1975. *Planta* 127, 121

Takala, H., H. Lehtivuori, H. Hammarén, V.P. Hytönen and J.A. Ihalainen. 2014a. Connection between absorption properties and conformational changes in *Deinococcus radiodurans* phytochrome. *Biochemistry*. 53(45):7076-7085

Takala, H., A. Björling, O. Berntsson, H. Lehtivuori, S. Niebling, M. Hoernke, I. Kosheleva, R. Henning, A. Menzel, J.A. Ihalainen and S. Westenhoff. 2014b. Signal amplification and transduction in phytochrome photosensors. *Nature*. 509:245-248

Terry M.J., Wahleithner, J.A, Lagarias J.C. 1993. *Arch. Biochem. Biophys*. 306, 1

Tu, S.L., and Lagarias J. 2005. in Handbook of photosensory receptors pp.121-149, *Wiley-VCH Press, Weinheim, Germany*

van Thor J. J., Borucki B., Crielaard W., Otto H., Lamparter T., Hughes J., Hellingwerf K. J., Heyn M. P. 2001. Light-induced proton release and proton uptake reactions in the cyanobacterial phytochrome Cph1. *Biochemistry* 40, 11460–11471

Vener S.J., Vierstra, R. D.1999. Bacteriophytochromes: phytochrome-like photoreceptors from nonphotosynthetic eubacteria. *Science* 286, 2517-2520

von Stetten, D., S. Seibeck, N. Michael, P. Scheerer, M.A. Mroginski, D.H. Murgida, N. Krauss, M.P. Heyn, P. Hildebrandt, B. Borucki and T. Lamparter. 2006. Highly conserved residues Asp-197 and His-250 in Agp1 phytochrome control the proton affinity of the chromophore and Pfr formation. *J Biol Chem*. 282(3):2116-2123

Wagner, J.R., J.S. Brunzelle, K.T. Forest and R.D. Vierstra. 2005. A light-sensing knot revealed by the structure of the chromophore-binding domain of phytochrome. *Nature*. 438:325-331

Wagner J.R., Zhang J., Brunzelle J.S., Vierstra, R.D., Forest,K.T. 2007. J. *Biol. Chem*. 282, 12298 –12309

Yang, X., Stojkovic, E. M., Kuk, J., Moffat, K. 2007. *Proc. Natl. Acad. Sci. U. S. A.* 104 12571–12576

Yang X., Kuk J., Moffat K. 2008. Crystal structure of Pseudomonas aeruginosa bacteriophytochrome: Photoconversion and signal transduction. *Proc. Natl. Acad. Sci. U.S.A.* 105, 14715–14720

Yang X., Ren Z., Kuk J., Moffat K. 2011. Temperature-scan cryocrystallography reveals reaction intermediates in bacteriophytochrome. *Nature* 479, 428–432

APPENDICES

Table A.1. **List of reagents and solutions used in the experiments**

Buffers used in protein purification	
Binding buffer	30 mM Tris pH 8.0, 150 mM NaCl, 5 mM Imidazole
Washing buffer	30 mM Tris pH 7.5, 150 mM NaCl, 10 mM Imidazole
Elution buffer	30 mM Tris pH 7.5, 150 mM NaCl, 500 mM Imidazole

SDS-PAGE gels

Lower gel (12 %)		Upper gel (4 %)	
8.0 ml	30 % acrylamide/bis solution 29:1	2.0 ml	30 % acrylamide/bis solution 29:1
2.8 ml	1.5 M Tris, pH 8.8	2.0 ml	0.5 M Tris, pH 6.8
0.1 ml	20 % SDS	0.1 ml	20 % SDS
2.5 ml	2 M sucrose	3.75 ml	2 M sucrose
6.6 ml	H_2O	7.0 ml	H_2O
133 µl	ammonium persulfate (APS) 100 mg/ml	138 µl	ammonium persulfate (APS) 100 mg/ml
20 µl	tetramethylethylenediamide (TEMED)	7,5 µl	tetramethylethylenediamide (TEMED)